

Chemisorption of a single oxygen molecule on the Si(100) surface: Initial oxidation mechanisms

Koichi Kato

*Advanced Materials and Devices Laboratory, Corporate Research and Development Center, Toshiba Corporation,
1 Komukai Toshiba-cho, Saiwai-ku, Kawasaki 210-8582, Japan*

Tsuyoshi Uda

Joint Research Center for Atom Technology, Angstrom Technology Partnership, 1-1-4 Higashi, Tsukuba, Ibaraki 305-0046, Japan

(Received 15 November 1999; revised manuscript received 19 June 2000)

Chemisorption of an O_2 molecule from the topmost layer to deeper subsurface layers on the Si(100) surface is studied by employing the spin-polarized generalized-gradient approximation. The calculated results reveal that an O_2 molecule is weakly adsorbed on a clean Si(100) surface with an initial spin-triplet state, but is adiabatically chemisorbed with a spin-state conversion, when an O_2 molecule arrives at the surface with a low incident energy. Barrierless back-bond oxidation has been found to occur through dissociative chemisorption with a spin-orbit interaction followed by O-atom migration to back-bond centers. According to the depth from the surface, energy barriers are found to be increasingly necessary for chemisorption of an O_2 molecule in subsurface layers.

I. INTRODUCTION

With the advent of silicon device technologies, the realization of a thin oxidized film of high quality on the Si(100) surface has emerged as an item of key interest in the context of achieving further progress in microscopic-scale device fabrication. The initial oxidation processes of the Si(100) surface are not, however, well understood despite considerable experimental and theoretical efforts. Much remains to be learned concerning the basic mechanisms inherent in initial oxidation processes of the Si(100) surface.

Regarding O_2 molecular chemisorption on the Si(100) surface, there have been contradictory reports, based on molecular-beam studies, as to the nature of the chemisorption.¹⁻⁷ The sticking probability of an O_2 molecule with a low incident energy increases with the lowering of temperature, whereas, surprisingly, that of an O_2 molecule with a high incident energy decreases with the lowering of temperature.³ The sticking probability of an O_2 molecule actually increases with decreasing incident energy.⁴ These phenomena can be understood to mean that O_2 molecule adsorption occurs through physisorption-mediated chemisorption at lower temperatures.^{3,4,7} This implies the existence of a molecular precursor just before oxidation and a small energy barrier for O_2 molecular chemisorption on the Si(100) surface. Recent scanning tunneling microscope (STM) studies showed, on the other hand, that the type-C defect⁸ is prone to oxidation, whereas clean (100) surfaces are not.^{9,10} This result indirectly supports the idea that there is a barrier of some sort against the oxidation of the clean Si(100) surfaces. The energy barrier for oxidation of the Si(100) surface has not been obtained, however. The mechanisms of this chemisorption and the consequent final configurations are also not well understood from these STM studies.

Another important subject is how to realize a precisely controlled interface structure between Si and SiO_2 when an oxidation process continues. A transition layer of less than 5 Å has been thought to move in a bulk phase of a Si substrate during the oxidation process, as clearly observed by the transmission electron microscope.¹¹ In a recent scanning re-

flection electron microscope (SREM) study,¹² it was found that layer-by-layer oxidation can be observed from the very beginning of subsurface layer oxidation in the low-temperature range of oxidation. These oxidation behaviors undoubtedly reflect differences in chemical processes of each subsurface layer, but those differences are not well understood from a microscopic viewpoint.

Several theoretical studies were devoted to elucidating the initial stages in Si surface oxidation processes.¹³⁻¹⁷ These calculations are insufficient to account for plausible physisorption-mediated chemisorption, and for the possibility of another dissociative chemisorption, which could have active roles mostly in the initial oxidation stage.^{3,4} Molecular dissociation of an O_2 molecule is triggered by breaking a delicate balance between two stable states. To clarify this issue, more rigorous treatments are required in theoretical studies. The ground states of an O atom and an O_2 molecule are paramagnetic spin-triplet states, which could make oxygen-involved reactions more complicated and, thus, more difficult to understand. Furthermore, accurate pathways in chemical reactions cannot be known without allowing the degree of freedom in spin state. The local-density approximation (LDA) does not provide accurate binding and cohesive energies for materials consisting of the first-row elements because of rapid spatial variation in wave functions by small atomic radius.¹⁸⁻²¹ In the present study, therefore, spin polarization and the generalized-gradient approximation (GGA) for exchange-correlation energies are applied. Based on these theoretical treatments, we have performed a first-principles study on spin-flip chemisorption of an O_2 molecule on Si surfaces, and have tried to understand general features in the initial oxidation processes on the Si(100) surface.²²

II. CALCULATION METHODS

The ground states of an O atom and an O_2 molecule are well known to be paramagnetic spin-triplet states with half-occupied $2p$ and $2p\pi_g^*$ orbitals, respectively. To describe the oxygen properties properly, the present study incorpo-

TABLE I. Binding energies (eV) of an O_2 molecule calculated with the LDA and SP-LDA in comparison with the experimental result (Expt).

Methods	LDA	SP-GGA	Expt ^a
	8.91	5.60	5.11

^aReference 27.

rates spin polarization and the GGA for exchange-correlation energies. Similar GGA calculations have proved to be successful in describing binding and cohesive energies for materials consisting of first-row elements.^{21,23} The present study implemented the Perdew formalism for spin-polarized GGA (SP-GGA) calculations.²⁴ The exchange-correlation potentials are discretized on the minimum number of fast-Fourier-transform grids within the plane-wave basis set by following the White-Bird formalism.²⁵ The calculations are performed using ultrasoft pseudopotentials, especially for oxygen,²⁶ with $2k$ points for the Brillouin-zone sampling. We found that cutoff energies of 25 Ry for the wave functions and 144 Ry for the augmented electron densities are sufficient for converging oxygen energies. The Si(100) surface is modeled as a repeated slab with a $c(4 \times 2)$ unit cell, consisting of ten layers of Si atoms and a vacuum spacing of the same thickness. Inversion symmetry with respect to the center of the slab is used to increase the computational efficiency.

To test the accuracy of this approach, the O_2 binding energy is calculated by using the calculation techniques of the LDA and the SP-GGA. Both spin-polarization and GGA effects contribute substantially to binding energies in comparison with the experimental result, as summarized in Table I. In the case of the LDA, the binding energy of 8.91 eV is almost 74% larger than the experimental value of 5.11 eV.²⁷ By employing the SP-GGA calculation, an O_2 binding energy of 5.60 eV is obtained. The discrepancy from the experimental value is reduced to 10%.

When an O_2 molecule moves toward the Si surface with a spin-triplet state, the spin-triplet potential curve crosses another potential energy with a spin-singlet state. The total system may be a singlet state when occupied states in oxygen are hybridized with Si substrate states. This triplet-to-singlet-state conversion actually occurs through a spin-orbit interaction, which is extremely weak compared to orbital hybridization energies. An adiabatic transition, therefore, only occurs when a molecule approaches the Si substrate slowly enough for the spin-orbit interaction to work. To describe the nonadiabatic transition at this spin conversion stage, we have applied the Landau-Zener-Stueckelberg theory.^{28,29}

III. RESULTS

Possible adsorption of an O_2 molecule is first examined by conserving the initial spin-triplet state on the Si(100)- $c(4 \times 2)$ surface. In all of the configurations studied in this work, the O_2 molecular axis is initially set parallel to the substrate surface, because this configuration makes the occupied molecular orbitals $2p\pi_u$ and the half-unoccupied molecular orbitals $2p\pi_g^*$ interact efficiently with the substrate. We have prepared seven initial configurations above the topmost layer for O_2 adsorption from (a) to (f) as shown

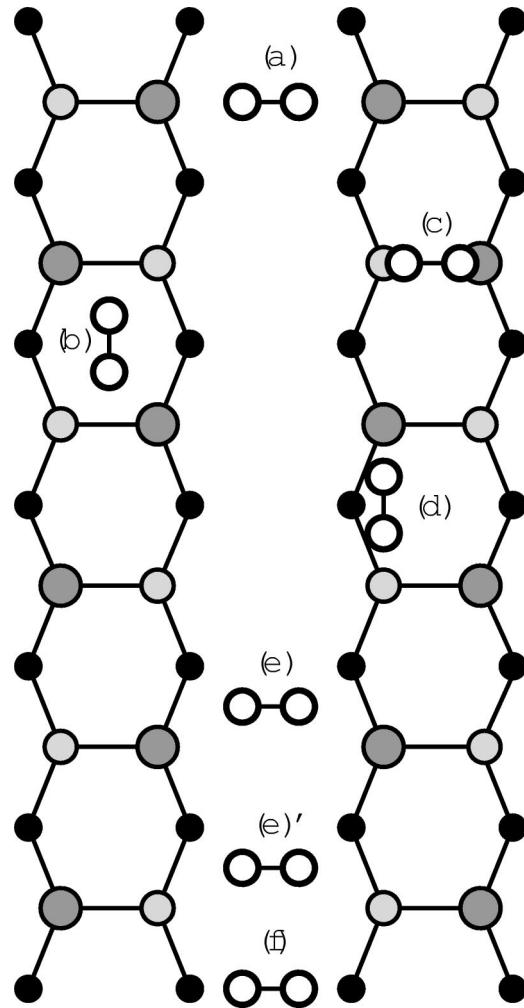


FIG. 1. Initial configurations of the (a), (b), (c), (d), (e), (e'), and (f) cases for O_2 molecular adsorption on the Si(100)- $c(4 \times 2)$ surface. Open circles are O atoms, and shaded and filled circles are Si atoms, respectively. Si atoms are denoted by larger to smaller circles according to the distance from the surface.

by open circles in Fig. 1. Since those sites from (a) to (d) are close enough to the highest occupied states on the upper atoms in a Si dimer, indicated by large shaded circles, a chemical reaction with the Si surface could be expected to occur. Then, we have selected three configurations (e), (e') and (f), as shown in Fig. 1, which are right above the bond center of first and second subsurface layers, respectively. Once an O_2 molecule was first put far from each selected site on the Si surface, the O and Si atoms were moved according to the forces acting on each atom, while the center of an O_2 molecule is artificially controlled to move toward the Si surface.³⁰

A. Spin-conserving weak adsorption (physisorption)

Figures 2(a)–2(d) show valence charge densities on cross sections of O_2 molecule adsorbed Si surfaces, corresponding to the initial configurations denoted by Figs. 1(a)–1(d). The valence charge densities of O and Si are slightly overlapped but do not show any mixing with each other in cases (a), (b), and (d), whereas the charge densities of O and Si in case (c) are rather strongly overlapped. However, neither elongation

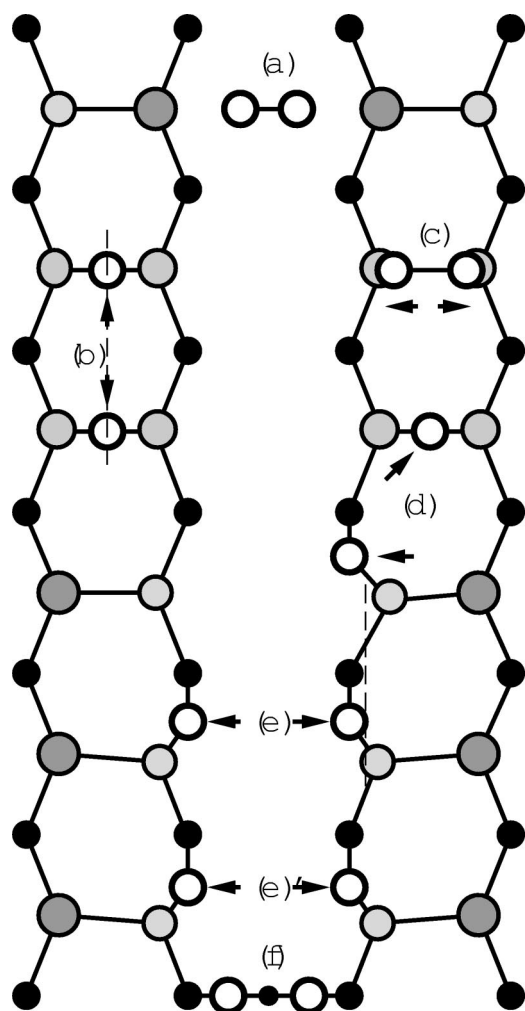


FIG. 3. Final configurations of the (a), (b), (c), (d), (e), (e)', and (f) cases for O_2 molecular adsorption on the Si(100)-c(4 \times 2) surface after molecules are dissociated and/or fully relaxed with spin-state conversion. Open circles are O atoms, and shaded and filled circles are Si atoms, respectively. Si atoms are denoted by larger to smaller circles according to the distance from the surface.

through spin-orbit interactions in a nonmagnetic system. The final configurations of cases (a) and (d) still remain unchanged from the initial configuration even if the spin state is allowed to change. Dramatic changes have been obtained in the cases (b) and (c) without overcoming any energy barrier. Figures 3(b) and 3(c) show the final configurations of O_2 molecular chemisorption corresponding to the cases (b) and (c) in Fig. 1. The corresponding valence-charge densities around the O atoms sliced along the dashed line and along the two atoms on the final configurations in Fig. 3 are shown in Figs. 4(b) and 4(c), respectively. Chemisorbed oxygen seems to be hybridized with electronic charges from the lower Si substrates. The energy changes for these reactions are also summarized in Table II.

In case (b), a molecule expands its bond length toward the adjacent parallel dimers, and is finally dissociated over the two Si dimers, corresponding to one of the stable configurations realized in the former LDA calculation.¹⁶ The dissociated O atoms settle down stably on the top of each Si dimer as shown in Fig. 3(b). The spin configuration results in a spin-singlet state. Asymmetric Si dimers below the O atoms

are also reformed to be symmetric. Here the O atoms and the lower Si atoms form strong chemical bonds. The energy gain is 5.99 eV. Since case (d), having a geometry closer to case (b), does not show any tendency toward chemisorption, dissociative chemisorption occurs where the two half-occupied antibonding $2p\pi_g^*$ states of an O_2 molecule are strongly hybridized with occupied states from two Si dimers in an appropriate geometry, and/or the O atoms make strong bonds with Si atoms by transferring electronic charges from Si atoms.

C. Chemisorption with energy barrier

There is some evidence that O atoms exist in back-bond centers upon oxidation at low temperatures as reported by the STM and SREM studies.^{12,31} If the topmost layers are fully oxidized, an O_2 molecule must be dissociated in lower subsurface layers or a dissociated O atom must migrate into the lower subsurface layers. To examine fundamental dissociation processes of an O_2 molecule with some energy barriers, the O_2 molecule is dissociated from cases (d), (e), (e)', and (f) of Fig. 1. Each O atom is moved toward a Si dimer or toward the adjacent Si bond center and is settled down between two Si atoms with a constraint on the center of an O_2 molecule mass fixed to move toward the Si substrate, as shown in Figs. 3(d), 3(e), 3(e)', and 3(f). Spin states are treated as one of the degrees of freedom. However, the dissociation of an O_2 molecule does not occur easily in case (a), although it is very close to two Si dangling bonds. In case (d), one of the dissociated O atoms finally settles down on the top of a Si dimer, and the other one in a back-bond center of a topmost Si atom. The dissociated O atoms finally settle down in bond centers of the first and second subsurface layers in cases (e), (e)', and (f), respectively. The final spin configurations are a spin-singlet state. These chemisorptions require the energy barriers of 0.8, 1.03, 0.29, and 2.4 eV in cases (d), (e), (e)', and (f), respectively, but obtain chemisorption energies of 6.16, 6.17, 6.59, and 6.00 eV in cases (d), (e), (e)', and (f), respectively, as tabulated in Table I. An important finding here is that a dimer chemisorbed with an O atom in a back-bond center always tilts downward from the Si surface at the O atom as shown in Figs. 3(e) and 3(e)'. The valence charge densities around O atoms on cross sections sliced along the two atoms [the dashed line in the final configurations for case (e)] is shown in Fig. 4(e). Chemisorbed oxygen seems to be hybridized with electronic charges from the lower Si substrates. O atoms chemisorbed on the topmost layer mostly settle down on the top of a Si dimer by breaking π orbitals of the Si dimer, whereas those chemisorbed on subsurface layers settle in the bond centers of two Si atoms by breaking Si σ orbitals. These are common features for O_2 molecule chemisorption processes. The fact that energy gains in cases (e) and (e)' are larger than those of cases (b) and (d) suggests that O atoms located in a bond center of two Si atoms is energetically the most stable configuration which can be realized in oxygen chemisorption.³²

D. Local densities of states

Our other concern is the mechanism for formation of Si-O bonds. As shown in Figs. 4(b)–4(e), O atoms chemisorbed

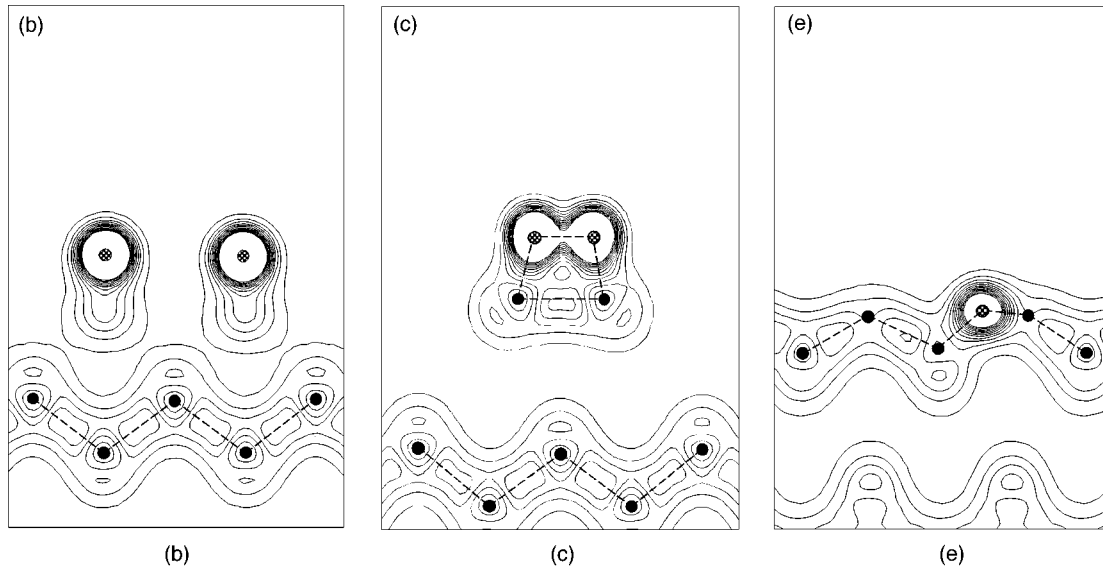


FIG. 4. Equicontour plots of valence-charge densities around O atoms sliced along the two O atoms in the final configurations of cases (b) and (c), and along the dashed line in the final configuration of case (e) of Fig. 3. O and Si atoms are indicated by hatched and dark circles, respectively.

on the top of a dimer or in a bond center seem to adsorb electronic charges from adjacent Si atoms. To arrive at a more detailed understandings of those mechanisms, we have calculated local densities of states (LDOS) around an O atom before and after dissociative chemisorption. Here we define the LDOS associated with each Wigner-Seitz cell. The supercell is divided into Wigner-Seitz cells. Then the LDOS at the O atom is calculated by summing the proportional volumes of electronic states involved in the Wigner-Seitz cell.

Figure 5(a) shows the LDOS of the O atom before dissociative chemisorption corresponding to Fig. 1(a) for comparison. We can observe three main peaks in this LDOS structure for each spin state. All the peaks are split into up- and down-spin states because the system is in a triplet state. The first peak, more than 25 eV below the Fermi level, corresponds to $2s\sigma_g$ orbitals. The second peak about 15 eV below the Fermi level corresponds to $2s\sigma_u^*$ orbitals. The third peaks around 10 to 0 eV from the Fermi level consist of $2p\sigma_g$, $2p\pi_u$, and $2p\pi_g^*$ orbitals. Those peaks undergo substantial changes upon the dissociative chemisorption. Figure 5(b) shows the LDOS at the O atom after chemisorption corresponding to Fig. 2(b). The peak consisting of $2s$ orbitals is almost degenerated because of molecular dissociation. This peak is not shifted much from the center of $2s\sigma_g$ and $2s\sigma_u^*$ orbital peaks in Fig. 5(a), although the O atom is negatively charged. The electronic charges in the Wigner-Seitz cell are actually summed as large as 6.3 electrons. The second peak around 5 eV from the Fermi level in Fig. 5(b) is not easy to split into three subpeaks, clearly featuring the characteristics of a hybridized orbital composed of oxygen $2p$ and silicon $3p$ orbitals rather than of an atomic orbital. Furthermore, we can see a broad peak corresponding to unoccupied antibonding states at higher energies above the Fermi level. Those results suggest that the dissociative chemisorption on this site occurs mostly by hybridization of atomic orbitals between the Si substrate and an O_2 molecule rather than by charge transfers from the Si substrate to an O_2 molecule. Figure 5(c) shows the LDOS at the O atom after

chemisorption corresponding to Fig. 3(e)'. The peak consisting of $2s$ orbitals is not shifted much from the center of $2s\sigma_g$ and $2s\sigma_u^*$ orbital peaks in Fig. 5(a), as well as in Fig. 5(b). The splitting of the second peak around 5 eV from the Fermi level in Fig. 5(b) is rather obscure to be identified. The electronic charges in the Wigner-Seitz cell are modest enough to be 6.5 electrons. The electronic states around O atom on the bond center also show rather strongly hybridized orbital characters. It implies that dissociation of an O_2 molecule and migration of an O atom in subsurface layers occur with rehybridization of atomic orbitals.

E. Migration of O atom from topmost layer to back-bond center

O atoms seem to be located in back-bond centers rather than on topmost layers when the Si substrate is exposed to O_2 molecular gas with submonolayer coverage,³¹ as the calculated results in the previous two subsections reveal that O atom chemisorption in bond centers gains more energies than that on the top of dimers. This means that O atoms may exist mostly at bond centers when the system comes close to a thermally equilibrated limit. So far, possible pathways of oxygens to reach back-bond centers are from cases (d), (e), and (e)' of Fig. 1 to those in Fig. 3. Another possible pathway for oxygen could be obtained by starting from O atoms dissociated on the top of a dimer as in cases (b) and (c) in Fig. 3.

Here, we examine the possible migration of O atoms on the top of dimers to lower back-bond centers. Cases (b) and (c) in Fig. 2 are chosen as typical initial configurations for O-atom migration because no energy barrier is required for the dissociative chemisorption. Figure 6 shows the energy change and schematic views of oxygen's rebonding processes during the migration in case (b). One of the two Si-O bonds is first remade to form double Si-O bonds, after overcoming an energy barrier of 1.27 eV, as listed in Table III. In this stage, a metastable geometry appears, where an O atom

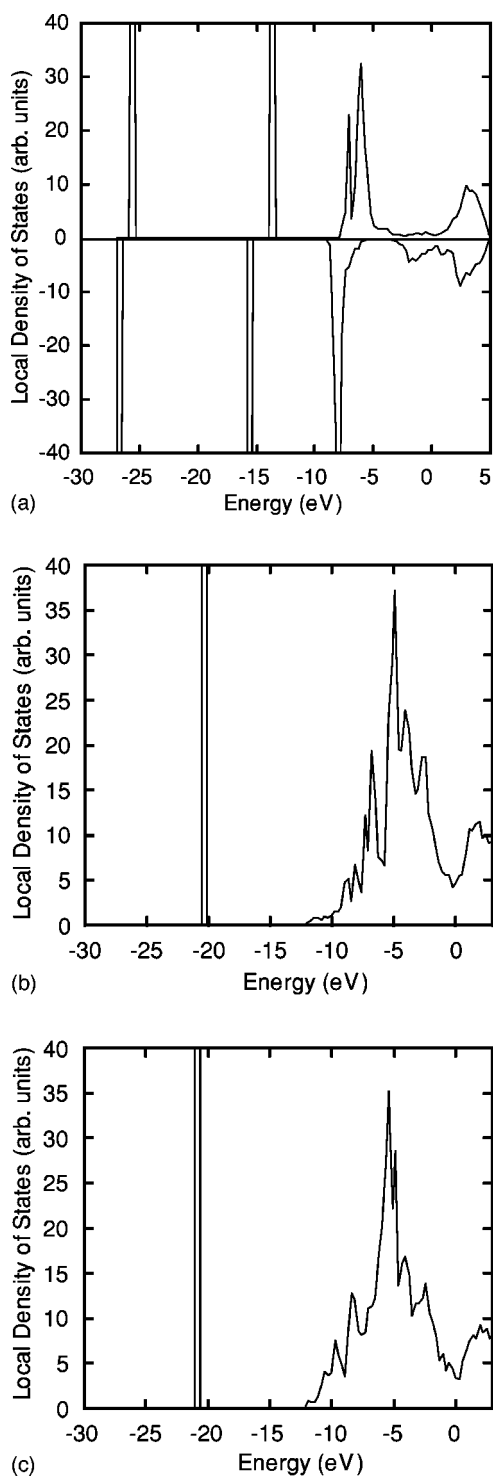


FIG. 5. Local density of states at the O atom (a) when an O_2 molecule is weakly adsorbed on the Si surface [case (a) of Fig. 1], (b) when an O atom is chemisorbed on the top of a Si dimer [case (b) of Fig. 3], and (c) when an O atom is chemisorbed at the back-bond center [case (e)' of Fig. 3].

is strongly bonded with one of the Si atoms in an asymmetric Si dimer. The energy gain in this metastable configuration is 0.63 eV from the top of the migration barrier. As the O atom moves further toward the lower bond center, another energy barrier of 0.50 eV, evaluated from the metastable configuration, appears. The final configuration comes upon a small energy gain of 0.17 eV from the first chemisorbed configu-

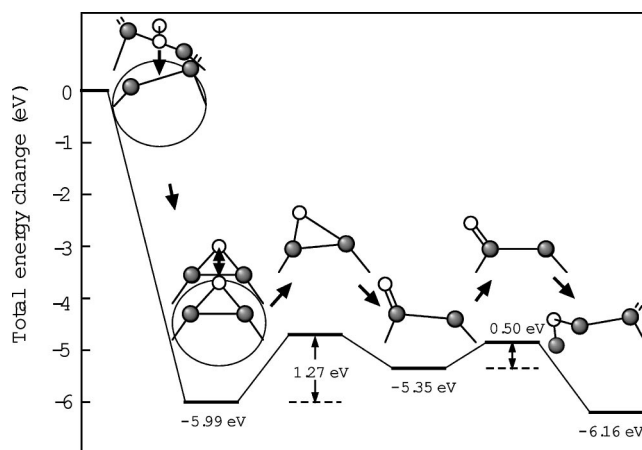


FIG. 6. Total-energy change and snapshots in geometry variation when a dissociated O atom, as in case (b) of Fig. 3 migrates from the top of a Si dimer to a back-bond center corresponding to case (d) of Fig. 3.

ration. The electric charges remained at the final configuration form a dangling bond on the Si atom opposite to the Si atom of a dimer chemisorbed with the O atom, which may be a chemisorption site for another O_2 molecule. In all the processes, two Si-O bonds have been remade, but the number of Si-O bonds has been maintained, leading to a relatively small energy barrier for O atom migration in comparison to hybridized bond energies between Si and O atoms.

Figure 7 shows the energy change and schematic views of oxygen's rebonding processes during the migration in case (c). The oxygen molecular bond is first broken with a strengthening of the Si-O bond. It requires a small energy barrier of 0.69 eV as listed in Table III. The O atom moves further toward the lower Si-Si bond center, where the O atom forms a strong bond with two Si atoms. In this stage, a metastable geometry appears, where the other O atom is bonded with one of the Si atoms on an asymmetric Si dimer. The energy gain in this metastable configuration is 3.02 eV from the top of the migration barrier. When the other O atom migrates from the top of the Si atom into the lower Si-Si back-bond center, it comes upon another energy gain of 1.56 eV after an energy barrier of 1.02 eV. The final configuration comes upon a substantial energy gain of 2.87 eV from the first chemisorbed configuration. It is obvious from these analyses that the O atom remaining at the top of a Si dimer could also exothermically migrate into a closer Si-Si bond center with a small energy barrier. By summarizing the analyses on these typical examples, we expect that migration occurs successively as a consequence of exothermic chemisorption of an O_2 molecule on Si surfaces.

TABLE III. Energy barriers and energy gains (eV) for O-atom migration from configurations (b) and (c) in Fig. 3 to a back-bond center.

Case	1st barrier	1st gain	2nd barrier	2nd gain	total gain
(b)	1.27	0.63	0.50	1.31	0.17
(c)	0.69	3.02	1.02	1.56	2.87

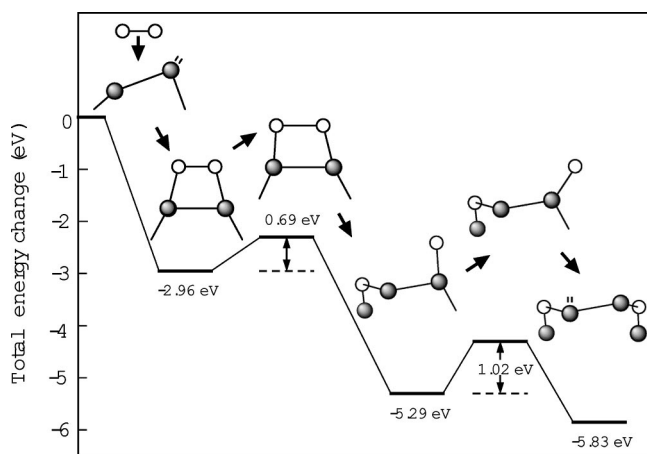


FIG. 7. Total-energy change and snapshots in geometry variation when a dissociated O atom, as in case (c) of Fig. 3 migrates from the top of a Si dimer to a back-bond center.

F. Spin conversion effects on chemisorption

As a spin state has been treated as one of the degrees of freedom required to find the minimum-energy configuration in the calculations for chemisorption, final-spin configurations are found to be part of a singlet state in any case of oxygen-chemisorbed Si(100) surfaces. Although final configurations after chemisorption are part of a spin-singlet state, the spin state has to be conserved in diabatic chemical processes in order for one to know the diabatic energy curves accurately. Dissociation pathways and energy barriers for the case (b) in Fig. 1 are, hereafter, examined closely as an instructive example of chemisorption, by taking account of the spin-conservation law. Each up- and down-spin electron number is conserved in a certain period along the potential energy curve. The O_2 molecule was lowered quasistatically toward the Si surface while maintaining the initial spin configuration. The total energy of the system is calculated as a function of the O-atom height from the Si surface for each spin state for case (b) in Fig. 3 as shown in Fig. 8.

A possible initial-spin configuration is a triplet, quintet, or singlet state when an O_2 molecule is put far above the Si surface. The lowest-energy initial configuration is a triplet state, as represented by triangles in Fig. 8, where an O_2 molecule and a Si surface are a triplet and a singlet state, respectively. The triplet state in this case corresponds to $S_z = 1$. The triplet states are represented by this state with $S_z = 1$ for energy curves, since the spin-orbit interaction is extremely small as compared to the exchange interaction. As the O_2 molecule moves with a constraint on the center of the molecular mass fixed toward the Si surface in the triplet case, this motion “finds” an upward valley on the potential-energy surface.²⁸ As the O_2 molecule approaches the Si surface, the triplet state crosses the energy curve of a singlet state. At the bond-breaking stage of the O_2 molecule, the O_2 molecule in a triplet state comes across an abrupt energy barrier blocking a further transition. The constraint by the triplet state causes an energy barrier preventing the O_2 molecule from coming closer to the Si surface. For the quintet state as represented by rectangles in Fig. 8, both the O_2 molecule and the Si surface are in a triplet state, and are coupled together in an antiparallel direction, when the O_2 molecule is

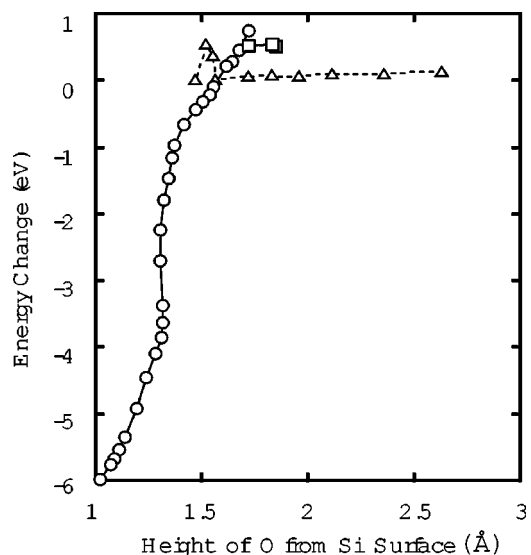


FIG. 8. Total-energy change as a function of O height from the Si surface when an O_2 molecule is dissociated as in case (b) of Fig. 3. Circles, triangles, and rectangles represent spin-singlet, spin-triplet, and spin-quintet configurations.

far from the Si surface and has no chemical interaction with the Si surface. We call this configuration a quintet state because the two systems have their own degrees of freedom in spin states, but it is finally a singlet state when the two systems are merged together, and loses its total spin because the quintet state with $S_z = 0$ immediately corresponds to a singlet state. One of the dimers closer to the O_2 molecule is relaxed until it is almost symmetric. In the spin-singlet state for the Si surface, up- and down-spin electrons occupy the same dangling bond on one side of one Si dimer. These electrons, however, half occupy the different dangling bonds on both sides of one Si dimer with the same up- or down-spins, when the Si surface is in a spin-triplet state. The total energy is relatively high, as much as 0.38 eV, compared with the total system in a spin-triplet state. As the O_2 molecule moves down to the Si surface, thereby slightly elongating the bond length, both spin configurations of the triplet states in the O_2 molecule and Si surface are converted into singlet states, and the total system remains a spin-singlet state, which is indicated by rectangles in Fig. 8. Then the half-occupied antibonding $2p \pi_g^*$ states in the O_2 molecule begin to hybridize with occupied states from dangling bonds on Si atoms. The bonds are remade to be strong σ_g bonds between O and Si atoms. After the O_2 bond-length elongation, this energy curve shows a lower energy than the triplet state for the total system. No apparent energy barrier appears along this transition. This configuration finally results in case (b) of Fig. 2. Another singlet state in the highest-energy configuration is represented by a circle, where both the O_2 molecule and the Si surface are in a singlet state. Therefore, both the O_2 molecule and the Si surface have no spin polarization. The total energy of this initial configuration is substantially high, as much as 1.14 eV, compared with the total system in a spin-triplet state at the initial stage. The motion of the O_2 molecule toward the Si surface leads to the same pathway as that obtained in calculations with a degree of freedom to the spin. The spin conversion first appears in an O_2 molecule and not in the Si surface. This case also results in case (b) of Fig. 2.

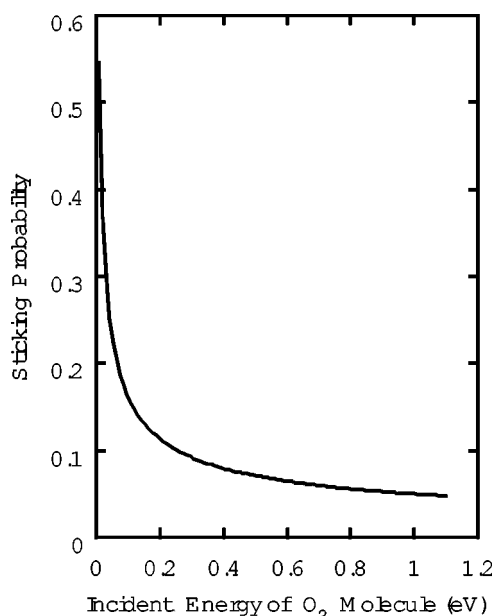


FIG. 9. Sticking probability as a function of incident energy of an O_2 molecule for case (e) of Fig. 3.

The energy curve crossing by the spin-triplet and spin-singlet states shown in Fig. 8 gives us a common feature unique to spin-flip O_2 chemisorption on Si(100) surfaces, although crossing angles may differ from site to site. The energy levels for both spin-triplet and spin-singlet states could be interchanged through spin-orbital interactions at the crossing points. When the spin-orbit interaction is perturbing in the range of two energy curve crossing points, the O_2 molecule in a spin-triplet state can be converted into a singlet state with a certain probability. The adiabatic spin conversion with a small perturbation at the energy-level crossing ranges can be described by applying the Landau-Zener-Stueckelberg theory. The probability for the $1 \rightarrow 2$ electronic transition is given by²⁸

$$P_{2 \leftarrow 1} = 4|D|^{-2} e^{2\pi\delta} (e^{2\pi\delta} - 1) \cos^2\left(\frac{\pi}{4} + \tau\right), \quad (1)$$

where δ is the imaginary part of a classical action integral, and τ is a phase factor. D is given by

$$D = e^{2\pi\delta} + (e^{2\pi\delta} - 1) e^{i[(\pi/2) + 2\tau]}. \quad (2)$$

Since the distance of Si and O atoms is great enough to be 2.7 Å, while the distance of two O atoms is 1.3 Å at the spin conversion stage, here we have calculated the transition probability with spin-orbit interactions in an O_2 molecule for simplicity. By using $\langle {}^1\Sigma_g^+ | H_{so} | {}^3\Sigma_g^- \rangle = 122 \text{ cm}^{-1}$ for the spin-orbit interaction,²⁹ $P_{2 \leftarrow 1}$ has been calculated as a function of the incident energy E_i of an O_2 molecule perpendicular to the surface, as shown in Fig. 9, where the oscillation factor is neglected. Sticking probabilities decrease with the incident energy in proportion to $E^{-1/2}$ at lower-energy ranges. The calculated curves well describe the overall tendency of incident energy dependence of sticking probabilities at low surface temperatures as clearly seen in the experiments of the molecular beam studies.⁴ The same discussion may be also applicable to case (c) of Fig. 3. A continuous

adiabatic-potential curve from the initial spin-triplet configuration to the final spin-singlet configuration is obtained by diagonalizing the Hamiltonian including spin-orbit interactions. The energy eigenvalues of the spin-triplet state at the initial configuration are split into three states after diagonalization. One of these three states, $L_z=0$ and $S_z=0$, lowest among the three states, could be adiabatically connected to the final spin-singlet state.²⁹ The above calculation implies that the adiabatic motion can be realized solely at lower temperatures and with lower incident energies for O_2 molecules. Translational motions or thermal vibrations of an O_2 molecule prevent the O_2 molecule from traveling with the adiabatic limit, because the energy perturbation by spin-orbit interactions in an O_2 molecule is too small to transfer between two energy curves. Those superfluous energies could break the adiabatic motion with a small spin-orbit splitting gap.

In case (c), a molecule is adsorbed in a weakly chemisorbed state, where the half-occupied orbitals in an O_2 molecule are hybridized with the occupied states of the Si surface. The final O_2 molecular bond length is elongated slightly with 0.30 Å. The asymmetric Si dimer below the O_2 molecule is also reformed to be symmetric to make bonds with the O_2 molecule, as seen from Fig. 4(c). A substantial energy gain of 2.96 eV is obtained in the final configuration. The charge densities between the O atoms and the Si atoms suggests that the antibonding $2p\pi_g^*$ orbitals of the O_2 molecule are hybridized with occupied states in the lower Si atoms, as seen from Fig. 4(c). The spin configuration results in a spin-singlet state. In this case, triplet to singlet conversion occurs at some point by charge transfer or hybridization of half-occupied oxygen orbitals and Si surface bonds. The spin-orbit interaction, therefore, also works here as the same mechanism works in case (b).

Since the final configurations for O_2 molecular chemisorption are spin-singlet states in any case, with certain energy barriers, conversion of a spin state may have some effect on chemical reactions, as is always true for barrierless chemisorptions in cases with no energy barriers. Diabatic energy curves for case (e) in Fig. 3 have been closely examined as an instructive example for chemisorptions with some energy barriers by conserving the spin state. Each up- and down-spin electron number is conserved in a certain period along the potential-energy curve. The total energy of the system is calculated as a function of the O-atom height from the top of the Si surface for each spin state. As shown in Fig. 10, an O_2 molecule starts to move toward the Si substrate with a stable spin-triplet state when an O_2 molecule is set far from a trough between two dimers on the Si surface. The energy barrier first appears at the initial stage of O_2 molecular dissociation, as represented by triangles representing the triplet state. Charge transfers may occur from dangling bonds on Si atoms to the O_2 molecule at the next stage. The spin state of the Si surface is converted into a triplet state, while that of the O_2 molecule is converted into a spin-singlet state. In these processes, the total spin configuration still remains in the initial triplet state. As the antibonding $2p\pi_g^*$ states in the O_2 molecule hybridize further with the remaining half-occupied states on the dangling bonds on Si atoms, a spin-singlet configuration represented by circles in Fig. 10 appears at an energy relatively lower than that of the spin-triplet configuration. The conversion from the spin-triplet

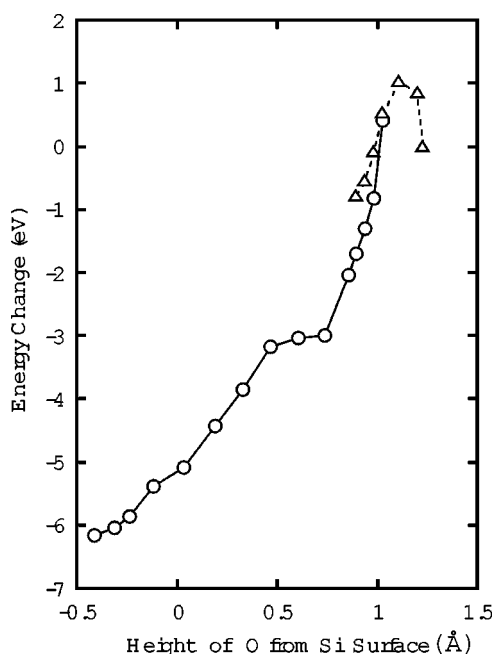


FIG. 10. Total-energy change as a function of O height from the Si surface when an O_2 molecule is dissociated as in case (e) of Fig. 3. Circles and triangles represent spin-singlet and triplet configurations.

state to the spin-singlet state eventually occurs after overcoming an energy barrier of 1.03 eV. Once the system overcomes the barrier, the entire system is inevitably converted into a spin-singlet state, because the trapped oxygens in a spin-triplet state could fall into an energetically lower singlet state. A spin-orbit interaction eventually works for spin-state conversion after the crossing points of the two energy curves, where another energy excitation is required for returning to the initial configuration. The activation energy to overcome the barriers is, therefore, most important for the chemisorption process in this case, rather than spin-state conversion, in contrast to the barrierless chemisorption in cases (b) and (c).

The energy-curve crossing also appears after a small energy barrier when an O_2 molecule is lowered inside a trough between dimers on the Si substrate in cases (e)' and (f) (not shown here). These are common features for dissociative chemisorption with some energy barriers.

IV. DISCUSSION

A. Chemisorption in initial stage

According to molecular-beam studies, the absolute values of the sticking coefficients of an O_2 molecule range from 2×10^{-4} to 0.2 at 300 K. This means that O_2 molecules with relatively low energies may be chemisorbed as a consequence of multiple collision events with the Si substrate. In particular, for lower incident energies, an O_2 molecule will have sufficient time to adjust its lateral position and molecular orientations before it is dissociatively chemisorbed, as observed in an O_2 molecule chemisorption on Pt and Ir surfaces.^{33,34} Another important mechanism is a spin-orbit interaction. As revealed in the present study, an O_2 molecule with a low incident energy is dissociatively chemisorbed

more easily through a spin-orbit interaction, whereas one with a slightly higher incident energy is repelled at the Si surface. Those general behaviors of adiabatic or diabatic processes, dependent on the incident molecular energies, are consistent with the findings of molecular-beam studies.^{3,4} The sticking coefficients for low incident energies were also found to increase with a lowering of the temperature.²

Since the incident energies of O_2 molecules used in the molecular-beam studies are at least 0.06 eV, these initial conditions for molecular energies may have given rise to some differences from STM studies. In STM studies,^{9,10} the Si substrate was exposed to O_2 molecular gas with a submonolayer coverage, mostly at temperatures slightly higher than room temperature. Direct dissociative chemisorption of an O_2 molecule at subsurface layers requires 0.8 or 0.29 eV for cases (d) or (e)' of Fig. 3. Since those processes require atomic motions in restricted configurations at and above room temperatures, they can occur with high incident energies or at high temperatures in the molecular-beam studies, but may not occur with low incident energies. A more plausible chemisorption pathway is the O_2 molecular dissociative chemisorption followed by migration of an O atom to a back-bond center, as described in relation to Fig. 6. This is because the initial chemisorption process generates a superfluous energy of almost 3 eV per O atom, which may successively cause oxygen migration with energy barriers of 1.27 or 0.6 eV. Another additive migration from a back-bond center to a lower bond center is unlikely to occur because it requires an energy barrier of 2.5 eV.^{35,36} The recent SREM observation of oxidation of the Si(100) strongly supports the idea that layer-by-layer oxidation starts from the first subsurface layer at room temperatures.¹² The activation energy of the first subsurface layer's oxidation has been found to be 0.03 eV, close to 0 eV. We cannot, of course, rule out the existence of dissociated O atoms on dimers, as shown in Fig. 3(b), because observation of a small chemisorbed O atom is not an easy task for STM. A chemisorbed O atom may eventually migrate from the top of a Si dimer to a back-bond center after long duration on a dimer. Surface protrusion on oxygen adsorbed substrates observed by the STM study³¹ may have been caused by buckling of dimers.³² In the present study, spontaneous dimer buckling is found to be caused by oxygen chemisorption in a back-bond center. These findings can account well the observations obtained by STM studies.

B. Oxidation in subsurface regions

As SREM observation of oxidation on the Si(100) indicates that layer-by-layer oxidation starts from the first subsurface layer at room temperatures,¹² the activation energy of the first subsurface layer's oxidation can be estimated to be very close to 0 eV. The STM study also implied O-atom chemisorption in a back-bond center at temperatures slightly higher than room temperatures.³¹ Direct correspondence of the SREM study to the STM study may be difficult, because the experimental conditions for these studies are not the same. However, those experimental results strongly indicate that oxidation proceeds from the first to the second subsurface layer in a layer-by-layer manner.

In our study, the activation energy of O₂ molecular dissociative chemisorption followed by O-atom migration from the topmost layer to the first subsurface layer is estimated as 0 eV. Since this process leaves a dangling bond on the opposite side of a dimer, another O₂ molecule arriving on the same adjacent parallel dimers can repeat the same dissociative chemisorption. Those processes thus fully oxidize the first subsurface layer without any barrier energy. The activation energies of O₂ molecular dissociative chemisorption on the second subsurface layer are estimated to be as large as 2.4 eV in the present study, accounting well for the experimental value of 2.5 eV for dissociative chemisorption at high temperatures.⁶ Although this dissociative chemisorption energy at the second subsurface layer does not directly correspond to the activation energy of oxidation at the second subsurface layer, these calculated results are in good accordance with the experimental results, where the second subsurface layer's oxidation requires an extremely long time or higher temperatures compared with that of the first subsurface layer. As the oxidation proceeds from the surface, the oxidized layers are expected to reduce the stress generated by volume expansion through lattice relaxation or amorphization. This process will substantially reduce the activation energy of the second layer's subsurface oxidation from the present dissociative chemisorption of 2.4 eV.

V. CONCLUSION

In conclusion, O₂ molecular adsorption is examined from several sites closer to the highest occupied state on the upper

atom in a Si dimer and above the subsurface bond centers. O₂ molecules are found to be weakly adsorbed with a spin-triplet state. The present studies also found that an O₂ molecule is adiabatically chemisorbed through a spin-orbit interaction at the center of adjacent parallel dimers or at the top of a dimer at lower temperatures when the O₂ molecule reaches the surface in an appropriate orientation with a lower incident energy. This dissociative chemisorption is followed by migration of an O atom from the topmost layer to a back-bond center, leading to a full oxidation of the first subsurface layer without any barrier energy. The dissociative chemisorption is also found to occur at sub-surface layers with a relatively higher incident energy, or at high temperatures. The calculated results explain well the existence of an O₂ molecular precursor, the sticking probabilities of an O₂ molecule reported in experimental studies, and the initial oxidation processes of Si subsurface layers.

ACKNOWLEDGMENTS

We are indebted to K. Terakura for a very helpful suggestion. The authors would like to thank T. Yamasaki and Y. Morikawa for their kind support, and also thank H. Katagiri and T. Uchiyama for useful discussions. The work was partly supported by the New Energy and Industrial Technology Development Organization (NEDO).

-
- ¹For a review of the interaction of oxygen and Si surfaces, see T. Engel, *Surf. Sci. Rep.* **18**, 91 (1993).
- ²M. P. D'evelyn, M. M. Nelson, and T. Engel, *Surf. Sci.* **186**, 75 (1987).
- ³T. Miyake, S. Soeki, H. Kato, T. Nakamura, A. Namiki, H. Kanba, and T. Suzuki, *Phys. Rev. B* **42**, 11 801 (1990); T. Miyake, A. Namiki, T. Takemoto, S. Soeki, H. Kato, H. Kanba, T. Suzuki, and T. Nakamura, *Jpn. J. Appl. Phys.* **29**, 723 (1990).
- ⁴B. A. Ferguson, C. T. Reeves, and C. B. Mullins, *J. Chem. Phys.* **110**, 11 574 (1999).
- ⁵U. Memmert and M. L. Yu, *Surf. Sci. Lett.* **245**, 185 (1991).
- ⁶M. L. Yu and B. N. Eldridge, *Phys. Rev. Lett.* **58**, 1691 (1987).
- ⁷H. Ibach, H. D. Bruchmann, and H. Wagner, *Appl. Phys. A: Solids Surf.* **29**, 113 (1982).
- ⁸R. J. Hamers and U. K. Kohler, *J. Vac. Sci. Technol. A* **7**, 2854 (1989).
- ⁹P. Avouris and D. Cahill, *Ultramicroscopy* **42-44**, 838 (1992).
- ¹⁰M. Udagawa, Y. Umetani, H. Tanaka, M. Itoh, T. Uchiyama, Y. Watanabe, T. Yokotsuka, and I. Sumita, *Ultramicroscopy* **42-44**, 946 (1992); M. Udagawa, M. Niwa, and I. Sumita, *Jpn. J. Appl. Phys.* **32**, 282 (1993).
- ¹¹A. Ourmazd, D. W. Taylor, J. A. Rentschler, and J. Bevk, *Phys. Rev. Lett.* **59**, 213 (1987).
- ¹²H. Watanabe, K. Kato, T. Uda, K. Fujita, M. Ichikawa, T. Kawamura, and K. Terakura, *Phys. Rev. Lett.* **80**, 345 (1998).
- ¹³S. Ciraci, S. Ellialtioglu, and S. Erkoc, *Phys. Rev. B* **26**, 5716 (1982).
- ¹⁴I. P. Batra, P. S. Bagus, and K. Hermann, *Phys. Rev. Lett.* **52**, 384 (1984).
- ¹⁵X. M. Zheng and P. V. Smith, *Surf. Sci.* **232**, 6 (1990).
- ¹⁶Y. Miyamoto and A. Oshiyama, *Phys. Rev. B* **41**, 12 680 (1990); **43**, 9287 (1991); Y. Miyamoto, *ibid.* **46**, 12 473 (1992).
- ¹⁷T. Hoshino, M. Tsuda, S. Oikawa, and I. Ohdomari, *Phys. Rev. B* **50**, 14 999 (1994); *Surf. Sci. Lett.* **291**, 763 (1993).
- ¹⁸O. Gunnarsson, J. Harris, and R. O. Jones, *J. Chem. Phys.* **67**, 3970 (1977).
- ¹⁹P. A. Serena, A. Baratoff, and J. M. Soler, *Phys. Rev. B* **48**, 2046 (1993).
- ²⁰F. W. Kutzler and G. S. Painter, *Phys. Rev. B* **45**, 3236 (1992).
- ²¹A. Garcia, C. Elsasser, J. Zhu, S. G. Louie, and M. L. Cohen, *Phys. Rev. B* **46**, 9829 (1992).
- ²²K. Kato, T. Uda, and K. Terakura, *Phys. Rev. Lett.* **80**, 2000 (1998).
- ²³Y. M. Juan and E. Kaxiras, *Phys. Rev. B* **48**, 14 944 (1993).
- ²⁴J. P. Perdew, in *Electronic Structure of Solids '91*, edited by P. Ziesche and H. Eschrig (Akademie Verlag, Berlin, 1991); J. P. Perdew and Y. Wang, *Phys. Rev. B* **45**, 13 244 (1992).
- ²⁵J. A. White and D. M. Bird, *Phys. Rev. B* **50**, 4954 (1994).
- ²⁶D. Vanderbilt, *Phys. Rev. B* **41**, 7892 (1990).
- ²⁷K. P. Huber and G. Herzberg, in *Molecular Spectra and Molecular Structure* (Van Nostrand Reinhold, New York, 1979).
- ²⁸See, for example, M. S. Child, *Mol. Phys.* **28**, 495 (1974).
- ²⁹S. R. Langhoff, *J. Chem. Phys.* **61**, 1708 (1974).
- ³⁰K. Kato, *Phys. Rev. B* **54**, 2210 (1996).

- ³¹R. Kliese, B. Rottger, D. Badt, and H. Neddermeyer, *Ultramicroscopy* **42-44**, 824 (1992).
- ³²T. Uchiyama and M. Tsukada, *Phys. Rev. B* **53**, 7917 (1996).
- ³³C. T. Rettner and C. B. Mullins, *J. Chem. Phys.* **94**, 1626 (1991).
- ³⁴D. Kelly, R. W. Verhoef, and W. H. Weinberg, *J. Chem. Phys.* **102**, 3440 (1995).
- ³⁵M. Ramamoorthy and S. T. Pantelides, *Phys. Rev. Lett.* **76**, 267 (1996).
- ³⁶Z. Jiang and R. A. Brown, *Phys. Rev. Lett.* **74**, 2046 (1995).